MRI Guided Surgical Planning and 3D Procedure Simulation for Partial Gland Cryoablation of the Prostate

Nicole Wake (nwake@montefiore.org)
Montefiore Hospital and Medical Center https://orcid.org/0000-0002-8441-6059
Andrew B. Rosenkrantz
NYU Langone Health
Daniel K. Sodickson
NYU Langone Health
Hersh Chandarana
NYU Langone Health
James S. Wysock
NYU Langone Health

Research

Keywords: prostate cancer, cryotherapy, 3D planning, MRI

Posted Date: February 14th, 2020

DOI: https://doi.org/10.21203/rs.2.23583/v1

Version of Record: A version of this preprint was published on November 3rd, 2020. See the published version at https://doi.org/10.1186/s41205-020-00085-2.

Abstract

Purpose This study reports on the development of a novel 3D surgical planning technique to provide pre-ablation treatment planning for partial gland prostate cryoablation (cPGA).

Methods Consecutive patients with magnetic resonance imaging (MRI)-visible (PI-RADS v2 score ≥ 3) and biopsy confirmed prostate cancer undergoing partial gland cryoablation (cPGA) (n=20) were prospectively enrolled in an IRB approved study investigating advanced methods of data visualization for treatment planning. All patients enrolled in the study underwent image segmentation of the prostatic capsule, index lesion, urethra, rectum, and neurovascular bundles based upon multi-parametric MRI data. Segmented imaging data were converted to 3D, 3D prostate models were viewed in computer-aided design (CAD) software, and virtual cryotherapy probes with -40°C isotherm volumes were created. Pre-treatment 3D prostate cancer models derived from MRI data were utilized to predict the number of and placement of cryotherapy probes to achieve confluent treatment volume. Treatment efficacy was measured with 6 month post-operative MRI, serum prostate specific antigen (PSA) at 3 and 6 months, and treatment zone biopsy results at 6 months were evaluated. Outcomes from 3D planning were compared to outcomes from a series of 20 patients undergoing cPGA using traditional 2D planning techniques.

Results The number of cryotherapy probes utilized matched the 3D plan in 16/20 (80%) of patients. 3D planning predicted a greater number of cryoprobes than 2D planning. Treatment zone biopsy was performed in 13/17 patients in the 3D cohort and was negative in 12 of these (92.9%). For the 3D group, 6 month biopsy was not performed in 4 (20%) due to undetectable PSA, negative MRI, and negative MRI Axumin PET. For the group with traditional 2D planning, treatment zone biopsy was positive in 3/14 (21.4%) of the patients, p = 0.056).

Conclusions 3D prostate cancer models derived from mpMRI data provide novel guidance for planning confluent treatment volumes for cPGA. This study prompts further investigation into the use of 3D treatment planning techniques.

Introduction

The relatively recent introduction of multiparametric magnetic resonance imaging (mpMRI) in the diagnostic paradigm for prostate cancer provides a critical improvement in disease localization; mpMRI of the prostate has emerged as the major imaging modality utilized to identify and characterize clinically significant prostate cancer [1–4]. Coupling mpMRI with targeted prostate biopsy [3, 5, 6]. Furthermore, this technique improves understanding of disease localization and extent within the gland, thus opening the possibility of targeted treatment via prostate gland ablation (PGA).

Although mpMRI can adequately identify prostate lesions, one major disadvantage of focal therapy for prostate cancer is that it is difficult to accurately determine the “kill” zone. While mpMRI accurately identifies disease location, it may underestimate precise tumor extent by approximately 30% [7]. Working

from radical prostatectomy specimens, Le Nobin et al reported that a treatment margin of approximately 13 mm around image visible disease was needed to ensure adequate disease capture [8].

Cryoablation of the prostate utilizes placement of trans-perineal needles (cryoprobes) under ultrasound guidance. Cryoprobes are placed into the prostate tissue using 2D image guidance for localization of prostate tumor. Tissue ablation is achieved through controlled development of an isotherm volume which is based upon the endothermic expansion of argon gas within the cryoprobe. The 3D size of the isotherm is limited by the length of the cryoprobe and coagulative tissue necrosis is executed through two rapid freeze-thaw cycles. Achieving a temperature of

-40°C ensures tissue destruction [16]. Monitoring of the ice ball and treatment temperatures is achieved via 2D ultrasound imaging and select placement of thermocouples. The success of partial gland prostate cryoablation (cPGA) depends upon the development of a 3D ablation volume that entirely encompasses the tumor and its margin within a zone of at least − 40 °C. Utilizing the correct number of cryoprobes in the correct spatial orientation is necessary to achieve this goal [9].

Manual treatment planning typically includes reviewing the pre-operative mpMRI to plan critical steps of the surgical procedure and anticipate potential complications. Surgeons mentally translate two-dimensional (2D) images into a three-dimensional (3D) image, but this is dependent on their spatial awareness and experience. This can be especially challenging in cases with irregular shaped lesions, where the treatment can be performed through a series of single probe ablations. If the surgeon's perspective is not consistent with the actual situation, this may lead to treatment failure or major complications. Reported outcomes for prostate cryoablation demonstrate positive biopsy rates from 12–38%[10–13]. Importantly, most existing data on cryoablation oncologic outcomes stems from treatment approaches that did not use mpMRI for disease localization. The major complication related to prostate gland cryotherapy is post-surgical erectile dysfunction with rates ranging from 45.3–93.0%; however, these complication rates stem from whole gland cryoablation as opposed to partial gland strategies [12, 14]. Other complications include urethral sloughing, urinary retention, incontinence, and urethral stricture [11, 13, 15]. With improved disease localization through mpMRI, limiting treatment to the precise tumor location limits the side effect profile of ablation [16]. The success of this treatment paradigm relies upon accurate disease targeting [17].

In order to overcome the shortcomings of 2D imaging techniques for pre-operative planning, 3D surgical planning has been applied in radiofrequency ablation [18–21] and liver cryotherapy [22]. Currently, commercial software relies upon 2D images and was developed for whole gland ablation and no commercial tools are available to guide treatment for partial prostate gland cryoablation (cPGA) in 3D. Developing a 3D confluent ablation zone that encompasses the image visible disease as well as the necessary treatment margin is critical to successful cPGA.

To address the inadequacies inherent to 2D mapping techniques, this study reports on the development of a novel 3D surgical planning technique to provide pre-ablation treatment planning for cPGA. Patient-specific 3D models based upon mpMRI are created and the cPGA procedure is simulated using virtual 3D

cryoprobes. Prior to cPGA, virtual 3D planning is utilized to confirm the required number and placement of cryoprobes to achieve confluent treatment volume for each unique lesion and margin. Optimization of the treatment plan in 3D by placing a predefined number of cryotherapy probes to best cover the lesion with the estimated − 40°C isotherm surface is expected to save time during the surgical procedure and to ultimately to help improve outcomes following cryotherapy for prostate cancer.

Methods

Patients with MRI-visible, biopsy proven prostate cancer (PI-RADS v2 score 3) scheduled to undergo cPGA (n=20) were enrolled in our Institutional Review Board approved prospective study investigating advanced methods of data visualization for patients with prostate cancer. Patient-specific 3D prostate cancer models were developed as described below. A comparison group (n=20) composed of men undergoing cPGA using 2D planning techniques was retrospectively evaluated. The patient demographics for the 2D and 3D planning groups are shown in Table 1.

	3D Planning	2D Planning	p-value
Age (years)			
Mean	65	66	0.71
Range	50-73	52-80	
PSA (ng/mL)	6.78 ± 4.02	6.42 ± 3.80	0.66
PI-RADs	3.86 ± 0.83	3.32 ± 0.82	0.03
Lesion volume (cm^3)	1.03 ± 1.61	0.38 ± 0.32	0.14

Table 1: Patient demographic information.

Patient-Specific 3D Prostate Cancer Models

Patient-specific 3D anatomical prostate cancer models that highlight the prostate, prostate tumor, urethra, neurovascular bundles, and rectal wall were created from the mpMRI data [23]. Regions of interest were segmented using Mimics 21.0 (Materialise, Leuven, BE) and visualized in 3D format with computer aided design (CAD) software (3-matic, Materialise, Leuven, BE).

Cryotherapy Probes

Virtual cryotherapy probes were designed using the 3-matic CAD software to emulate the -40º C isotherm volumes from published dimensions. Virtual -40º C isotherms were created for 1.5cm, 2.5cm, 3.0cm, 4.0cm, and 5.0cm cryoprobe volumes **(Figure 1)**.

3D Surgical Planning/Simulations

Virtual treatment simulation was performed in the 3-matic software pre-treatment for all patients in the 3D planning group and retrospectively post-treatment for the 2D planning group. The 3D prostate model was oriented in a supine position allowing the simulation to be performed in the same alignment as the cPGA operating procedure and a 1cm margin was created around each tumor. Virtual cryotherapy probes were then selected and manually placed into the software in a spatial orientation to ensure confluent -40 º C isotherm encompassing both the tumor and the margin. This model was assessed in multiple views to ensure treatment confluence. The distances between the center of each probe were measured in order to reproduce the plan during the operation. In addition, contours of the anatomy and selected cryotherapy probes were generated on the 2D MR images.

Operating Procedure

All cryoablation procedures were performed under general anesthesia in a dorsal lithotomy position. A BK Flexfocus 800 biplanar ultrasound probe (model # 8808) attached to a Civco brachytherapy stand and stepper was utilized to visualize the prostate. Healthtronicsä cryoablation equipment was utilized to perform all ablations procedures.

2D Planning Method:

For patients undergoing treatment with 2D planning, the Healthtronics^{TM} software package was utilized to plan probe location. This software utilizes a 2D rigid registration of the prostate in an axial view on ultrasound. Probe placement is then guided by the 2D software in order to optimize probe-to-probe distance, probe-to-capsule distance, and probe -to

urethra distance. This software does not utilize any MR-US fusion technology. MR tumor location is targeted using visual estimation. Visual estimation is performed preoperatively using image measurements on axial and sagittal MR images. These measurements are translated to real-time US imaging to achieve visual estimation in lesion targeting. Cryotherapy probes are then placed under axial and sagittal ultrasound guidance. Each needle is placed via a 16 gauge brachytherapy grid with 2.5 mm distance between each grid location.

3D Planning Method:

The same software and equipment as described above is utilized for 3D planning with the exception of the pre-treatment planning as described above. The location of the pre-planned cryoprobes are then placed according to the 3D treatment planning, also using visual estimation. Again, no fusion software was available on the ultrasound for these ablation procedures. *Cryoablation Procedure:*

After completing cryoablation needles according to the treatment plan, thermocouples are placed into specific treatment locations in order to provide real-time temperature monitoring of critical locations including treatment margins and safety monitors. Cystoscopy is then performed to ensure that no needles traverse the urethra. A urethral warming catheter is then placed. The cryoablation cycle is then initiated. Freezing proceeds from anterior needles to posterior glands. Propagation of the ice is monitored using ultrasound imaging in axial and sagittal views. Treatment efficacy is further assessed with real-time evaluation of thermocouple temperature to ensure achievement of target temperature in the treatment zone and to maintain sufficiently warm temperatures in critical regions such as the rectum and external sphincter. Two freeze-thaw cycles were performed. The total freeze time and nadir temperatures were recorded. Operating times were also recorded for patients. A Students t-test was performed to determine if there was a difference between 2D and 3D planning groups (Matlab 2017a, The Mathworks Inc, Natick, MA). The number of cryotherapy probes planned was compared to the number utilized.

Evaluation of Treatment

In order to measure treatment efficacy, treatment zone biopsy results at 6 months were evaluated. Post-operative MRI and PSA at 3 and 6 months were also performed. The Kruskal-Wallis H Test was performed to determine if there was a difference in positive biopsy rates for the 2D and 3D planning groups. Statistical evaluation was carried out in SPSS Software (IBM, Armonk, NY).

Results

The 3D surgical plan was successfully simulated in all 20 patients selected to undergo pre-procedural 3D planning. 3D planning for a representative patient is shown in Fig. 2 and contours of this 3D plan are shown overlaid onto the 2D T2-Weighted MR images in Fig. 3.

All patients in the 3D planning group successfully underwent the focal cryotherapy procedure following the 3D surgical simulation. The number of cryotherapy probes utilized matched the plan in 16/20 patients (80%). For the four patients where the plan did not match the actual amount utilized, more cryoprobes were utilized in three cases and fewer cryobrobes were utilized in one case. Discrepancy in planned to utilized cryoprobes resulted from anatomical restrictions (gland size, inability of place needles as planned via grid). For the group with only 2D planning, 3D plans were performed retrospectively for 18/20 patients (90%). The number of probes in the 3D plan matched the number utilized for 5/18 patients (27.78%), predicted that more probes should be utilized for 10/18 patients (55.56%), and predicted fewer probes for 3/18 patients (16.67%). The average number of cryoprobes utilized was 4.10 ± 1.37 and 3.25 ± 0.44 for the groups with 3D pre-operative planning and only 2D planning respectively. Operating times were recorded for 15 patients with retrospective 2D planning and 14 patients with prospective 3D planning. The mean operating times were 100.47 ± 24.30 and 100.64 ± 13.19 minutes for the 2D and 3D groups respectively ($p > 0.05$).

For the 3D planning group, 18 patients returned for follow-up. Biopsy was not performed in 4 of these patients: two patients with undetectable PSA, one patient with MRI negative findings and PSA = 0.58, and one patient with negative hybrid PET/MRI. For the remaining 14 patients, biopsy results at 6 months were negative for 13 patients (92.9%). The single patient who was positive for cancer post-operatively had a 450mm^3 lesion and the number of cryoprobes planned matched the number utilized (n = 4). Post treatment MRI was available in all patients and demonstrated ablation zone completely encompassing pre-treatment MR lesion in 18/20 (90%).

For the 2D planning group, 13 returned for follow-up biopsy. Of these, ten (76.9%) had negative 6 month post ablation biopsy. Three patients (23.1%) were positive in the ablation zone, one patient with Gleason score 3 + 3 in the medial margin and two with Gleason score 3 + 4 in the treatment zone. Of these

patients, the predicted plan using 3D modeling matched the actual plan in once case (4 cryoprobes for both) and predicted more cyroprobes in two cases. For these cases, three cryoprobes were utilized, but one 3D plan predicted 5 cryoprobes but only 3 were utilized and the other predicted that 4 cryoprobes would be necessary to cover the target volume. Although 3 patients had positive findings post-operatively in the 2D planning group as compared to one patient in the 3D planning group, this did not reach statistical significance ($p = 0.056$). No post-surgical complications were reported for either group.

Discussion And Conclusions

Prostate cancer is the most common cancer in American men, accounting for almost 1 in 5 new cancer diagnoses annually [24]. The majority of prostate cancer is diagnosed following a screening evaluation of serum PSA followed by prostate biopsy [25]. The widespread use of this diagnostic paradigm most often identifies prostate cancer at an early stage when it is localized to the prostate gland [25–27]. Early identification of the disease allows for multiple management strategies, including surveillance for low grade disease and whole gland radiation and radical prostatectomy for intermediate and high-risk disease. Due to significant treatment toxicities associated with both radiation and radical prostatectomy, partial gland ablation (PGA) for prostate cancer aims to achieve oncologic control while mitigating side effects by limiting treatment to only regions of known cancer and preserving normal surrounding tissue.

Multiple technologies have been employed for focal therapy including high-intensity focused ultrasound (HIFU), cryotherapy, electroporation, radiofrequency ablation, and photodynamic therapy [28–32]. While an organ sparing strategy is widely employed in multiple oncologic treatments including kidney and breast cancer, employing this approach for prostate cancer has been limited by challenges in precise determination of tumor location and volume within the prostate gland [33].

Multi-parametric MRI is increasingly utilized for detection, localization, and staging of prostate cancer and offers a potential tool for image guided PGA of prostate cancer [34, 35]. Despite this significant advance, achieving a confluent “kill zone” for MRI-guided PGA remains a significant challenge. In this study, we report the use of 3D prostate cancer models used in conjunction with mpMRI and advanced 3D visualization software methods to plan and simulate a theoretic zone of cryoablation for image-guided cryotherapy ablation of prostate cancer.

The pre-operative 3D prostate cancer models are helpful in planning the cryotherapy procedure. These 3D models easily conceptualize the location of the tumor within the prostate as well as provide guidance on the extent of the necessary treatment margin (in this study a 1 cm margin was utilized) to predict an adequate “kill” zone. The 3D models also provide a comprehensive understanding of the 3D surgical anatomy including an understanding of the relationship of surrounding critical structures to the proposed treatment zone.

The virtual cryotherapy probes also allowed the exact “kill zone” to be predicted pre-operatively, thereby facilitating the operating procedure. The procedure was successfully carried out in all patients following the 3D virtual surgical planning procedure. In regards to the cryotherapy probe selection, there was a

strong correlation between the planned number and the actual number used in the surgical procedure (80%), which suggests that the 3D surgical plan helped to guide the procedure. Although there was no difference in operating times between groups, less variation was seen in the 3D planning group. In addition, in this small cohort, a greater number of patients in the 3D planning group were negative for cancer post-operatively as compared to those in the 2D planning group, with 1/17 (5.9%) and 3/13 (23.1%) positive for cancer at follow-up biopsy for the 3D and 2D groups respectively. The fact that 3D planning predicted a greater number of cryoprobes than 2D planning and that there was a higher success rate in the 3D cohort suggests that 3D planning allows for a more comprehensive assessment of the coverage area needed for successful tumor ablation. Future studies with more patients will assess how this method of procedure simulation compares to traditional 2D planning with mpMRI and how it impacts long-term treatment efficacy.

Conclusions

This study represents a preliminary exploration of a novel 3D treatment planning approach to cPGA of the prostate. Meaningful differences between 3D planning and traditional 2D planning were not possible in this study due to the small cohort and retrospective nature of the evaluation; however, the results encourage additional study in a larger cohort.

Declarations

Ethics approval and consent to participate

This study was approved by the NYU Langone Health Institutional Review Board (IRB). All patients signed written informed consent to participate.

Consent for publication

- All authors provided consent for publication

Availability of data and materials

- The datasets used and/or analyzed during the current study are available from the corresponding author on reasonable request.

Funding:

- Grant Support: NIH P41 EB017183

- In-Kind Support: Stratasys

Authors' Contributions:

- NW – Experimental design, imaging, patient recruitment, 3D modeling, pre-surgical virtual simulations, data analysis, manuscript writing, manuscript editing
- ABR –Experimental design, imaging, 3D modeling, manuscript editing
- DKS – Experimental design, imaging, manuscript editing
- JSW – Experimental design, patient recruitment, pre-surgical virtual simulations, data analysis, manuscript writing, manuscript editing
- HC - Experimental design, imaging, 3D modeling, manuscript editing

Competing interests:

- Financial Disclosures related to this work: none
- Financial and Non-Financial Disclosures not related to this work:
  - NW - In-Kind Research Support: Stratasys, Ltd.
  - ABR – Royalties, Thieme Medical Publishers, Inc.
  - DKS – Royalties, General Electric Company License agreement, General Electric Company; Royalties, Bruker Corporation License agreement, Bruker Corporation; Research collaboration, Siemens AG
  - HC – Equipment support, Siemens AG; Software support, Siemens AG; Advisory Board, Siemens AG; Speaker, Bayer AG.
- No competing interests: JSW

References

1. Bratan F, Niaf E, Melodelima C et al. Influence of imaging and histological factors on prostate cancer detection and localisation on multiparametric MRI: a prospective study. *Eur Radiol* 2013; **23**: 2019-29.
2. Haffner J, Lemaitre L, Puech P et al. Role of magnetic resonance imaging before initial biopsy: comparison of magnetic resonance imaging-targeted and systematic biopsy for significant prostate cancer detection. *BJU international* 2011; **108**: E171-8.
3. Meng X, Rosenkrantz AB, Mendhiratta N et al. Relationship Between Prebiopsy Multiparametric Magnetic Resonance Imaging (MRI), Biopsy Indication, and MRI-ultrasound Fusion-targeted Prostate Biopsy Outcomes. *European urology* 2016; **69**: 512-7.

4. Villers A, Puech P, Mouton D et al. Dynamic contrast enhanced, pelvic phased array magnetic resonance imaging of localized prostate cancer for predicting tumor volume: correlation with radical prostatectomy findings. *The Journal of urology* 2006; **176**: 2432-7.
5. Siddiqui MM, Rais-Bahrami S, Turkbey B et al. Comparison of MR/ultrasound fusion-guided biopsy with ultrasound-guided biopsy for the diagnosis of prostate cancer. *JAMA* 2015; **313**: 390-7.
6. Kasivisvanathan V, Rannikko AS, Borghi M et al. MRI-Targeted or Standard Biopsy for Prostate-Cancer Diagnosis. *N Engl J Med* 2018; **378**: 1767-77.
7. Priester A, Natarajan S, Khoshnoodi P et al. Magnetic Resonance Imaging Underestimation of Prostate Cancer Geometry: Use of Patient Specific Molds to Correlate Images with Whole Mount Pathology. *The Journal of urology* 2017; **197**: 320-6.
8. Le Nobin J, Rosenkrantz AB, Villers A et al. Image Guided Focal Therapy for Magnetic Resonance Imaging Visible Prostate Cancer: Defining a 3-Dimensional Treatment Margin Based on Magnetic Resonance Imaging Histology Co-Registration Analysis. *The Journal of urology* 2015; **194**: 364-70.
9. Baust JG, Gage AA, Bjerklund Johansen TE, Baust JM. Mechanisms of cryoablation: clinical consequences on malignant tumors. *Cryobiology* 2014; **68**: 1-11.
10. Caso JR, Tsivian M, Mouraviev V, Polascik TJ. Predicting biopsy-proven prostate cancer recurrence following cryosurgery. *Urol Oncol* 2012; **30**: 391-5.
11. Jones JS, Rewcastle JC, Donnelly BJ et al. Whole gland primary prostate cryoablation: initial results from the cryo on-line data registry. *The Journal of urology* 2008; **180**: 554-8.
12. Long JP, Bahn D, Lee F et al. Five-year retrospective, multi-institutional pooled analysis of cancer-related outcomes after cryosurgical ablation of the prostate. *Urology* 2001; **57**: 518-23.
13. Barqawi AB, Huebner E, Krughoff K, O'Donnell CI. Prospective Outcome Analysis of the Safety and Efficacy of Partial and Complete Cryoablation in Organ-confined Prostate Cancer. *Urology* 2018; **112**: 126-31.
14. Caso JR, Tsivian M, Mouraviev V et al. Complications and postoperative events after cryosurgery for prostate cancer. *BJU international* 2012; **109**: 840-5.
15. Han KR, Cohen JK, Miller RJ et al. Treatment of organ confined prostate cancer with third generation cryosurgery: preliminary multicenter experience. *The Journal of urology* 2003; **170**: 1126-30.
16. Ahmed HU, Dickinson L, Charman S et al. Focal Ablation Targeted to the Index Lesion in Multifocal Localised Prostate Cancer: a Prospective Development Study. *European urology* 2015; **68**: 927-36.
17. Guillaumier S, Peters M, Arya M et al. A Multicentre Study of 5-year Outcomes Following Focal Therapy in Treating Clinically Significant Nonmetastatic Prostate Cancer. *European urology* 2018; **74**: 422-9.
18. Altrogge I, Kroger T, Preusser T et al. Towards optimization of probe placement for radio-frequency ablation. *Medical image computing and computer-assisted intervention : MICCAI International Conference on Medical Image Computing and Computer-Assisted Intervention* 2006; **9**: 486-93.

19. Ren H, Campos-Nanez E, Yaniv Z et al. Treatment planning and image guidance for radiofrequency ablation of large tumors. *IEEE J Biomed Health Inform* 2014; **18**: 920-8.
20. Baegert C, Villard C, Schreck P, Soler L. Multi-criteria trajectory planning for hepatic radiofrequency ablation. *Medical image computing and computer-assisted intervention : MICCAI International Conference on Medical Image Computing and Computer-Assisted Intervention* 2007; **10**: 676-84.
21. Villard C, Soler L, Gangi A. Radiofrequency ablation of hepatic tumors: simulation, planning, and contribution of virtual reality and haptics. *Comput Methods Biomech Biomed Engin* 2005; **8**: 215-27.
22. Jaberzadeh A EC. Pre-operative planning of multiple probes in three dimensions for liver cryosurgery: comparison of different optimization methods. *Mathematical Methods in the Applied Sciences* 2016; **39**: 4764-72.
23. Wake N, Chandarana H, Huang WC et al. Application of anatomically accurate, patient-specific 3D printed models from MRI data in urological oncology. *Clin Radiol* 2016; **71**: 610-4.
24. Siegel RL, Miller KD, Jemal A. Cancer Statistics, 2017. *CA: a cancer journal for clinicians* 2017; **67**: 7-30.
25. Litwin MS, Tan HJ. The Diagnosis and Treatment of Prostate Cancer: A Review. *JAMA* 2017; **317**: 2532-42.
26. Hayes JH, Barry MJ. Screening for prostate cancer with the prostate-specific antigen test: a review of current evidence. *JAMA* 2014; **311**: 1143-9.
27. Eggener SE, Cifu AS, Nabhan C. Prostate Cancer Screening. *JAMA* 2015; **314**: 825-6.
28. Arumainayagam N, Moore CM, Ahmed HU, Emberton M. Photodynamic therapy for focal ablation of the prostate. *World J Urol* 2010; **28**: 571-6.
29. Cordeiro ER, Cathelineau X, Thuroff S et al. High-intensity focused ultrasound (HIFU) for definitive treatment of prostate cancer. *BJU international* 2012; **110**: 1228-42.
30. Djavan B, Susani M, Shariat S et al. Transperineal radiofrequency interstitial tumor ablation (RITA) of the prostate. *Tech Urol* 1998; **4**: 103-9.
31. Tsivian M, Polascik TJ. Focal cryotherapy for prostate cancer. *Curr Urol Rep* 2010; **11**: 147-51.
32. Valerio M, Stricker PD, Ahmed HU et al. Initial assessment of safety and clinical feasibility of irreversible electroporation in the focal treatment of prostate cancer. *Prostate Cancer Prostatic Dis* 2014; **17**: 343-7.
33. Marshall S, Taneja S. Focal therapy for prostate cancer: The current status. *Prostate Int* 2015; **3**: 35-41.
34. Kersten-Oertel M, Jannin P, Collins DL. The state of the art of visualization in mixed reality image guided surgery. *Comput Med Imag Grap* 2013; **37**: 98-112.
35. Muller BG, van den Bos W, Brausi M et al. Role of multiparametric magnetic resonance imaging (MRI) in focal therapy for prostate cancer: a Delphi consensus project. *BJU international* 2014; **114**: 698-707.

Figures

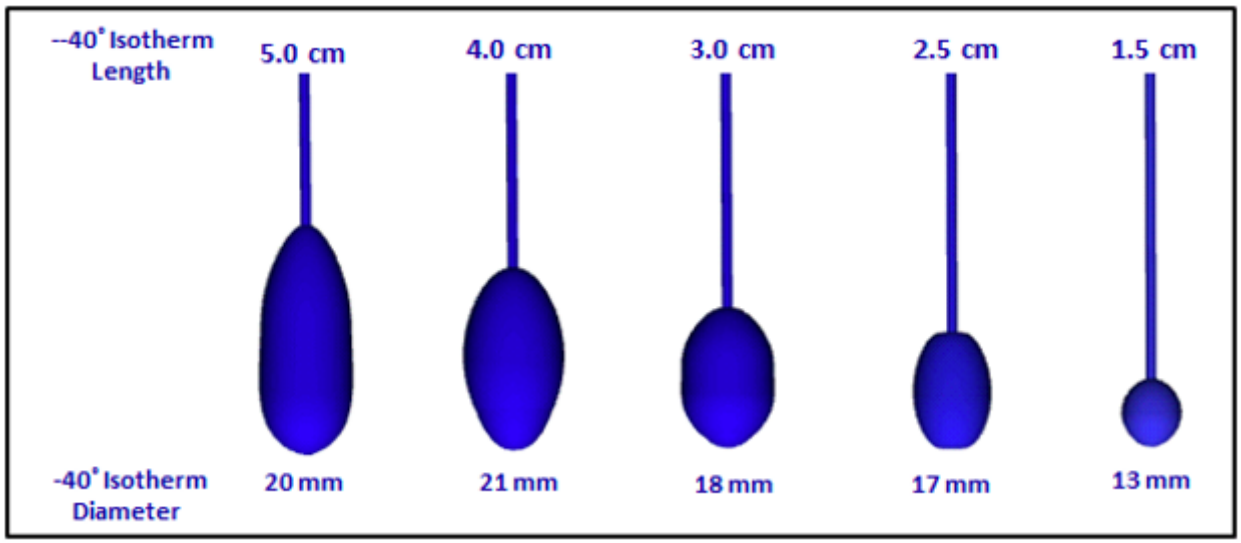

Figure 1

3D virtual cryotherapy probes of multiple dimensions to simulate different -40º ice-ball dimensions.

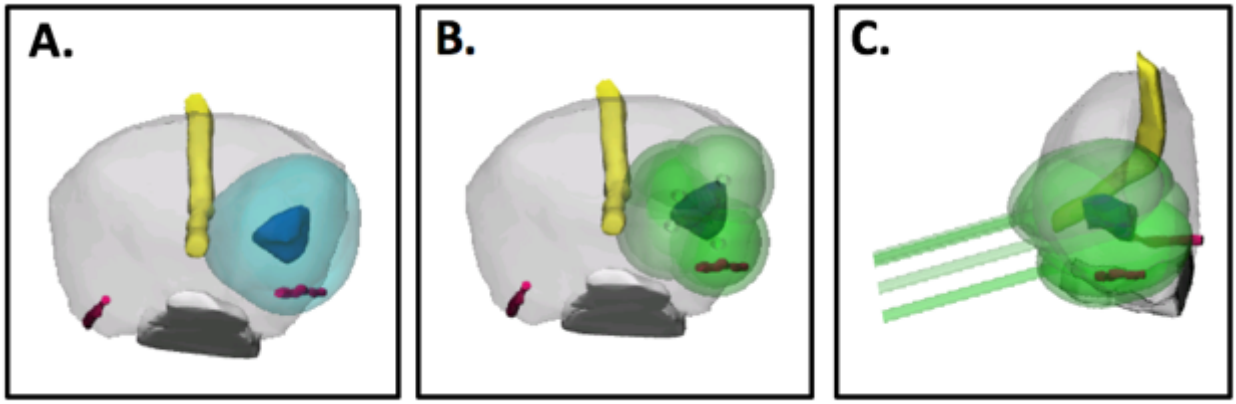

Figure 2

A. 3D prostate cancer model viewed from the apex (prostate – light gray, urethra – yellow, neurovascular bundles – pink, rectal wall – white, tumor – dark blue, tumor with 1cm margin – cyan). B. 3D model from A shown with probe placement. C. Sagittal view of model with probe placement.

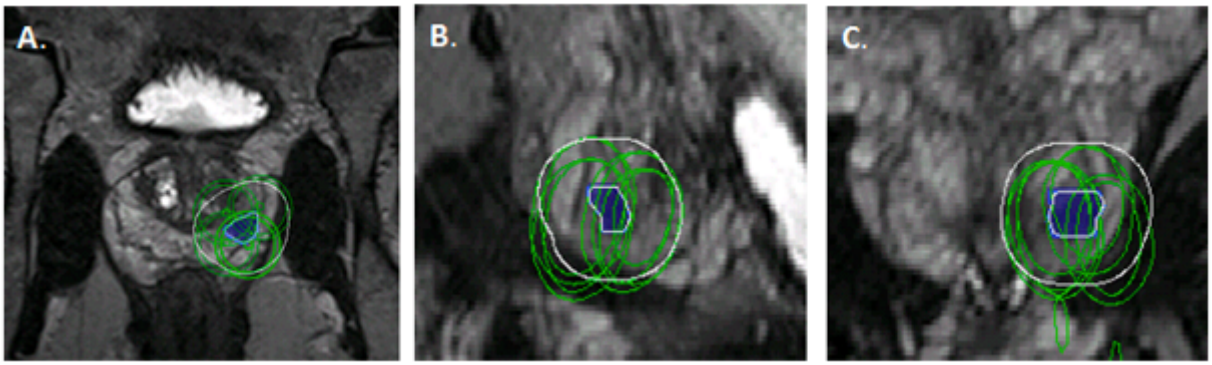

Figure 3

A) Axial, B) Sagittal, and C) Coronal images from 3D T2-Weighted MR sequence with the lesion (blue), outline of the 1cm margin (white), and outline of the cryotherapy probes (green).